Numerical and simplified methods for soil-pile interaction analysis

Carbonari S. [1], Dezi F. [2], Leoni G. [3], Morici M. [3]

[1] Università Politecnica delle Marche; s.carbonari@univpm.it
[2] University of San Marino; francesca.dezi@unirsm.sm
[3] University of Camerino; michele.morici@unicam.it; graziano.leoni@unicam.it

ABSTRACT

The paper presents a review of the analytical and numerical procedures developed by the authors for the dynamic analysis of soil-pile foundation systems subjected to the propagation of seismic waves in the soil. Inclined and vertical single piles and groups constituted by piles with a generic inclination are addressed. For the former, an analytical approach based on the beam on dynamic winkler foundation approach is adopted; the pile is modelled as a Euler-Bernoulli beam and the soil-pile interaction is captured by defining soil impedances relevant to the harmonic vibrations of rigid disks available in the literature. The coupled flexural and axial behaviour of the pile is solved analytically exploiting exponential matrices. The pile group dynamic problem is similarly formulated but the solution is achieved exploiting the finite element approach. Besides numerical models, simplified approaches based on static equivalent methods and simplified formulas are also addressed to estimate the maximum kinematic stress resultants on vertical piles subjected to lateral seismic excitations. The reliability of the presented tools in capturing the dynamic stiffness and the overall kinematic response of pile foundations is shown by comparing results with those available in the literature or achieved through refined finite element models. From an engineering point of view, the proposed approaches assure a sufficient accuracy and may substitute refined computational demanding numerical models.

1 INTRODUCTION

Damage sustained during past earthquakes has highlighted that the seismic behavior of structures and infrastructures is highly influenced by the response of the soil-foundation system. For this reason, modern seismic codes have started, at least in particular cases, to address the design and the verification of the structure, its foundation and the local deposit as a whole system. The substructure method plays a significant role for performing soil-structure interaction analysis allowing the analysis of the soil-foundation and superstructure subsystems separately and a more easily identification of their dynamic behaviours through the use of dedicated software. In the framework of the substructure method, the dynamic response of soil-foundation systems in the case of deep foundations can be studied with different approaches: *i*) elastic continuum methods, in which the soil is considered as an elastic medium [e.g. 1-3]; *ii*) Winkler-type (or p-y curves) methods, which, in their more refined versions, can also account for nonlinear soil behaviour in the vicinity of the pile shaft [e.g. 4-8]; *iii*) finite and boundary elements, and finite difference methods in both frequency domain [e.g. 9-12] or time domain to account for soil non linearity [e.g. 13-15]. In addition, when soil-structure interaction analyses are not required and only kinematic interaction effects on piles have to be computed, simplified approaches available in the literature can be used [e.g. 16-21].
The goal of this paper is to present a general overview of the analytical and numerical procedures developed by the authors for the dynamic analysis of soil-pile foundation systems subjected to the propagation of seismic waves in the soil. Both single piles and pile groups with general layouts (including also inclined piles) embedded in homogeneous as well as in inhomogeneous soil profiles are addressed. In the first section, an analytical approach based on the beam on dynamic Winkler foundation approach for the dynamic analysis of inclined and vertical single piles is presented; the pile is modelled as a Euler-Bernoulli beam and the soil-pile interaction is captured starting from local soil-pile impedances available in the literature. The coupled flexural and axial behaviour of the pile is solved analytically exploiting exponential matrices. In the second section, the dynamics of pile groups subjected to the propagation of seismic waves is formulated and the solution achieved through the finite element approach. Besides numerical models, simplified approaches based on static equivalent methods and simplified formulas are also presented in both sections (i.e. for single piles and pile groups) to estimate the maximum kinematic effects on piles. The procedures presented herein may be used in practice or in research to obtain realistic estimation of the dynamic impedances, the Foundation Input Motion (FIM) and stress resultants along piles.

2 SINGLE PILES

2.1 Analytical approach

In this section an analytical approach for the kinematic interaction analysis of inclined single piles, based on the Beam on Dynamic Winkler Foundation approach is addressed, and an analytical solution is derived. The pile is modelled as a Euler-Bernoulli beam having a generic inclination and the soil-pile interaction is captured by defining soil impedances according to expressions available in the literature for viscoelastic layers undergoing harmonic vibrations of a rigid disk. The coupled flexural and axial behaviour of the pile is described by a system of partial differential equations, with the relevant boundary conditions, that is solved analytically exploiting exponential matrices.
The dynamic problem of the single pile of diameter d and length L embedded in a homogenous soil deposit and subjected to the free-field seismic displacements is formulated in the frequency domain by assuming a linear behaviour for the pile and soil (Figure 1a). A Euler-Bernoulli model is assumed for the pile that is constituted by a linear viscoelastic material, characterized by Young's modulus E_p and material damping δ_p, considered according to the correspondence principle [22]. During the motion, the pile interacts with the surrounding soil without developing gaps and resultants of the soil reactions $\boldsymbol{r}$ are assumed to be constituted by line forces distributed along the pile axis (Figure 1b); by considering the soil stratum constituted by infinite horizontal independent layers with linear viscoelastic behaviour, the compatibility condition between the pile and soil displacements, due to both the free-field motion and the soil-pile interaction forces (Figure 1c), make it possible to express forces $\mathbf{r}$ as

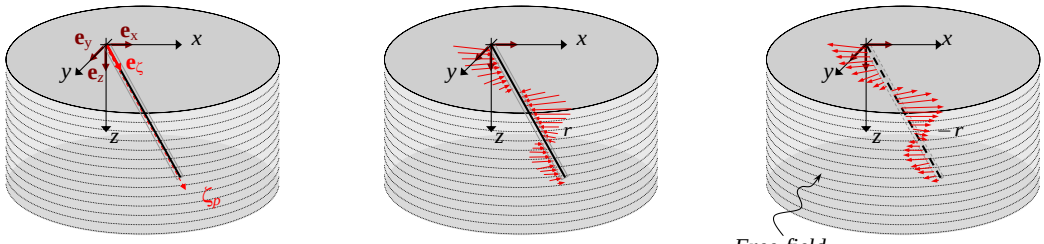

Figure 1. (a): Pile section in the homogeneous stratum; (b) pile section subjected to interaction forces and (c) soil stratum subjected to propagating seismic waves and interaction forces.

$$\mathbf{r}(\omega\,;z) = \boldsymbol{\mathcal{K}}(\omega)\left\{\begin{bmatrix}\mathbf{u}_{ff,h}(\omega\,;z)\\ u_{ff,z}(\omega\,;z)\end{bmatrix} - \begin{bmatrix}\mathbf{u}_{h}(\omega\,;z)\\ u_{z}(\omega\,;z)\end{bmatrix}\right\} \tag{1}$$

where ω is the circular frequency, $\mathbf{u}_{ff,h}$ and $u_{ff,z}$ are the grouped horizontal and vertical components, respectively, of the free-field motion and $\boldsymbol{\mathcal{K}}$ is the 3x3 impedance matrix of the unbounded soil layers. Furthermore, $\mathbf{u}_h$ and u_z are the grouped horizontal and vertical components of the pile axis displacements at depth z, expressed with respect to a global reference system (Figure 1a).
Matrix $\boldsymbol{\mathcal{K}}$ can be populated considering results of studies by Dobry et al. [23], Makris and Gazetas [24] and Gazetas and Dobry [25]; its components represent forces necessary to induce unitary harmonic vibrations of a rigid disk at depth z. The equilibrium condition of the pile may be expressed by the Lagrange-D'Alembert principle that, suitably integrated by parts, furnishes the following local balance conditions, expressed with respect to the pile local reference system

$$\begin{aligned}
&E_p^*\mathbf{J}\mathbf{u}_t'''' + \omega^2\rho_p\mathbf{J}\mathbf{u}_t'' - \omega^2\rho_p A\mathbf{u}_t + c_{z\zeta}\coprod_{1,2}^{1,2}(\mathbf{R}\boldsymbol{\mathcal{K}}\mathbf{R}^{\boldsymbol{T}})\mathbf{u}_t + c_{z\zeta}\coprod_{1,2}^{3}(\mathbf{R}\boldsymbol{\mathcal{K}}\mathbf{R}^{\boldsymbol{T}})\,u_\zeta = c_{z\zeta}\coprod_{1,2}^{1,2}(\mathbf{R}\boldsymbol{\mathcal{K}})\mathbf{u}_{ff,h} + c_{z\zeta}\coprod_{1,2}^{3}(\mathbf{R}\boldsymbol{\mathcal{K}})\,u_{ff,z}\\
&-E_p^*A\mathbf{u}_t'' - \omega^2\rho_p A u_\zeta + c_{z\zeta}\coprod_{3}^{1,2}(\mathbf{R}\boldsymbol{\mathcal{K}}\boldsymbol{R}^{\boldsymbol{T}})\mathbf{u}_t + c_{z\zeta}\coprod_{3}^{3}(\mathbf{R}\boldsymbol{\mathcal{K}}\mathbf{R}^{\boldsymbol{T}})\,u_\zeta = c_{z\zeta}\coprod_{3}^{1,2}(\mathbf{R}\boldsymbol{\mathcal{K}})\mathbf{u}_{ff,h} + c_{z\zeta}\coprod_{3}^{3}(\mathbf{R}\boldsymbol{\mathcal{K}})\,u_{ff,z}
\end{aligned} \tag{2}$$

with the relevant boundary conditions

$$\begin{aligned}
&\left(E_p^*Au_\zeta' + F_\zeta\right)\hat{u}_\zeta\big|_0 = 0\ \ \forall\hat{u}_\zeta && \left(E_p^*Au_\zeta' - F_\zeta\right)\hat{u}_\zeta\big|_L = 0\ \ \forall\hat{u}_\zeta\\
&\left(E_p^*\mathbf{J}\mathbf{u}_t''' + \omega^2\rho_p\mathbf{J}\mathbf{u}_t' - \mathbf{F}_t\right)\cdot\hat{\mathbf{u}}_t\big|_0 = 0\ \ \forall\hat{\mathbf{u}}_t && \left(E_p^*\mathbf{J}\mathbf{u}_t''' + \omega^2\rho_p\mathbf{J}\mathbf{u}_t' + \mathbf{F}_t\right)\cdot\hat{\mathbf{u}}_t\big|_L = 0\ \ \forall\hat{\mathbf{u}}_t\\
&\left(E_p^*\mathbf{J}\mathbf{u}_t'' + \mathbf{M}_t\right)\cdot\hat{\mathbf{u}}_t\big|_0 = 0\ \ \forall\hat{\mathbf{u}}_t' && \left(E_p^*\mathbf{J}\mathbf{u}_t'' - \mathbf{M}_t\right)\cdot\hat{\mathbf{u}}_t\big|_L = 0\ \ \forall\hat{\mathbf{u}}_t'
\end{aligned} \tag{3}$$

In Equations (2) and (3), $\mathbf{J}$ is the inertia matrix and A is the area of the pile cross section, respectively, while $E_p^*=E_p(1+2i\xi_p)$ is the complex elastic modulus of the pile material [22]; $\mathbf{u}_t$ and u_ζ are the grouped horizontal and vertical pile displacement components expressed with respect to the pile local reference system whose longitudinal axis ζ has direction cosine $c_{z\zeta}$ (Figure 1a). Furthermore, $\coprod_{i,j}^{l,m}\blacksquare$ is an operator indicating segments of a generic matrix constituted by the subset of rows comprised between i and j and the subset of columns comprised between l and m, and $\mathbf{R}$ is the rotation matrix which allows that allows expressing the local displacements starting from the relevant global quantities. Finally, in Equation (3), $\mathbf{F}_t$ and F_ζ are the transverse and longitudinal forces, respectively, while $\mathbf{M}_t$ is the vector collecting transverse moments applied at the pile ends ($\zeta = 0$ and $\zeta = L$).
Equations (2) is a system of ordinary differential equations with constant coefficients describing the coupled flexural-axial dynamic behaviour of the inclined pile. Unknowns are the complex valued function $\mathbf{u}_t(\zeta)$ and $u_\zeta(\zeta)$ fulfilling Equations (3) that encompass both kinematic and static boundary conditions. Solution of system (2) is provided in Appendix I for the one-dimensional propagation of shear and pressure waves in the vertical direction. Displacements at the pile head represents the motion at the foundation level (i.e. the FIM) while the soil-pile complex impedance matrix $\boldsymbol{\mathfrak{I}}$ can be obtained through the condensation of the soil-pile stiffness matrix on the pile head displacements. The latter, which represents forces necessary to induce unit-amplitude harmonic displacements at the pile head, is classically used in the framework of the sub-structure approach to define compliant restraints of superstructures in the inertial interaction analysis.
Differently from classical numerical methods (e.g. finite element method and finite difference method), this approach allows expressing the problem solution analytically; in the case of homogeneous soil deposit the discretization of the pile axis is not needed to achieve an accurate numerical solution, although some numerical issues relevant to the computation of the exponential matrix may require the pile axis subdivision into segments of limited length [8]. In the case of layered soil deposits, the problem can be solved exploiting solution provided in Appendix I for the homogenous deposit; assuming uniform soil properties within each layer, a different solving system is assembled for each pile segment belonging to the homogenous layer and suitable boundary conditions are provided at the pile head, at the pile base and at the interface between layers, where the pile continuity (with both reference to kinematic and static issues) has to be imposed. A similar approach can be adopted for the computation of impedance functions. Alternatively, the finite element method can be exploited: the stiffness matrix is assembled considering contributions of the pile segments (provided in Appendix I) and external forces are obtained assembling those resulting at the ends of each segment, obtained from the system solution assuming homogeneous boundary conditions. With this approach, impedances of the soil-pile system descend directly from the condensation of the dynamic stiffness matrix on the pile head degree of freedom [8].
In the sequel few applications are presented to demonstrate the model potential in capturing the dynamic response of inclined piles in terms of impedance functions, kinematic response factors and pile stress resultants, considering results obtained from a Boundary Element (BE) formulation available in literature. Further details and validation analyses can be found in [5]. In detail, pile

configurations adopted by Padron et al. [26] and Medina et al. [27] are considered (Figure 2) for what concern impedance functions and kinematic response factors. Figure 2 shows a comparison between the impedance functions obtained with the proposed model and those available in [26]; non-dimensional components of the impedance matrix (i.e. the translational $\Im_x$, vertical $\Im_z$, rotational $\Im_{\varphi y}$ and coupled roto-translational $\Im_{x-\varphi y}$ components) are plotted in the same frames as a function of the non-dimensional frequency $a_0 = \omega d/V_s$, being V_s the shear wave velocity of the soil. Furthermore, d is the pile diameter while E_p and E_s are the pile and soil Young's moduli, respectively. Concerning horizontal impedance in the x direction, it can be observed that real parts are reproduced well for both stiff (E_p/E_s = 100) and soft (E_p/E_s = 1000) soils while some inaccuracies characterise the imaginary parts; the latter are generally overestimated in the whole frequency range. Vertical impedances are well captured with only some slightly differences for the damping coefficients (10%). Rotational impedance around axis y (orthogonal to the plane of inclination) are well reproduced for vertical or slightly inclined piles while errors up to 25% appears for θ = 30° and soft soil conditions. Finally, the roto-translational behaviour is affected by some slightly inaccuracies. As for displacements, the kinematic response of the soil-foundation systems subjected to vertically steady propagating shear waves in planes xz and yz (Figure 2), scaled to have unit displacement amplitude at the ground surface, is analysed.

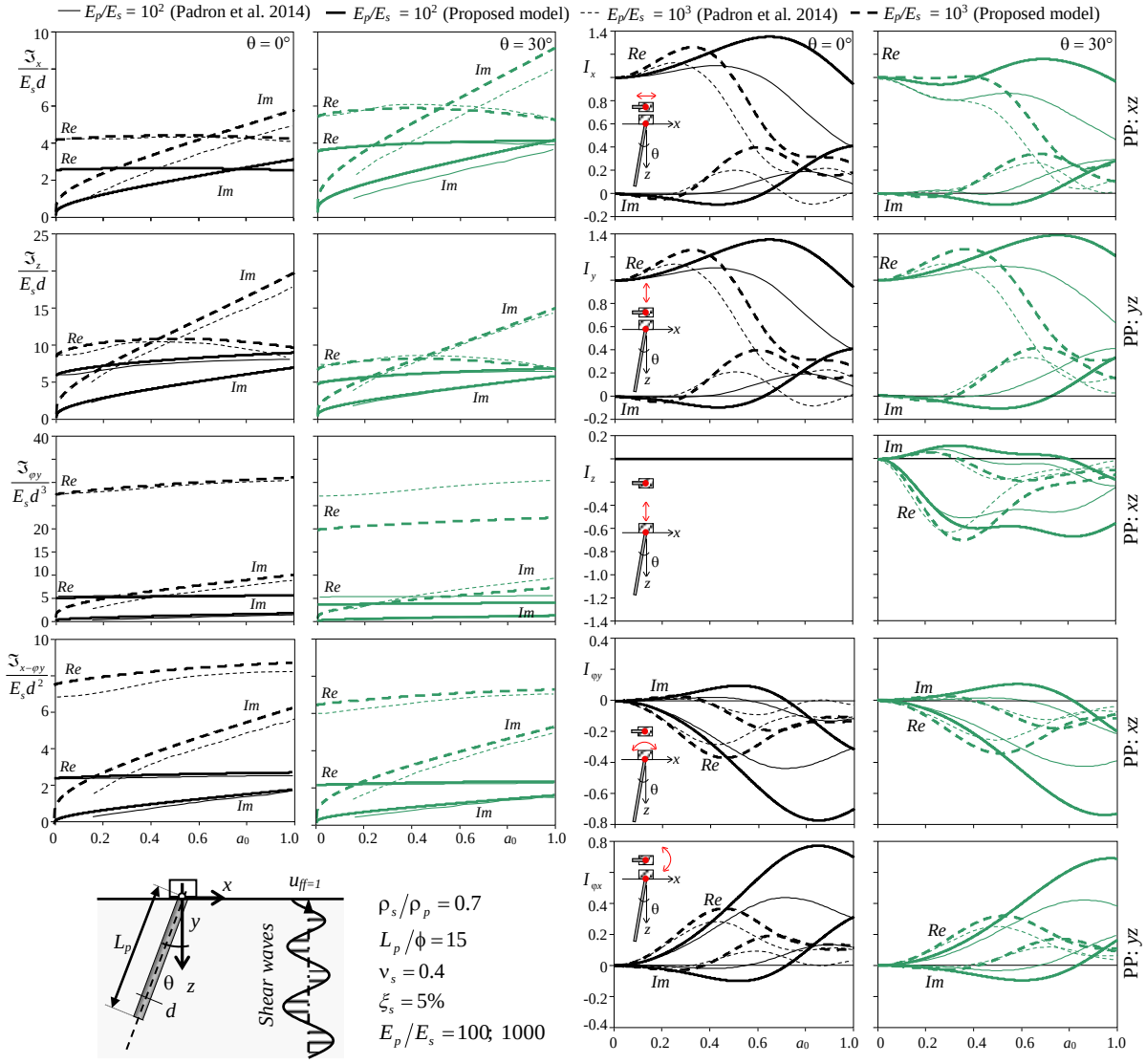

Figure 2. Case studies and comparisons of impedances and kinematic response factors with results from literature

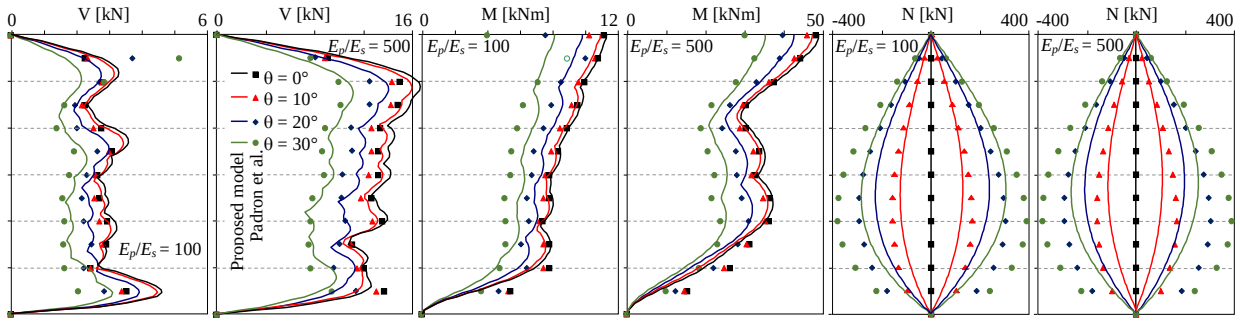

Figure 3. Envelopes of stress resultants: comparisons with results from literature

Figure 2 shows the comparison between the non-dimensional kinematic response factors (i.e. the translational I_x, I_y, I_z, and rotational $I_{\varphi y}$, $I_{\varphi x}$ components) [28] (curves with thick lines) evaluated and results available in [27] (curves with thin lines). The overall trend of results reveals that the response obtained with the presented model is overestimated with respect to results of a BE approach; in particular, at high non-dimensional frequency the response is sensibly over-predicted in the case of stiff soils (E_p/E_s = 100) with errors up to 100%.
This is probably due to the adopted local soil-pile impedances, which are derived starting from the plain-strain condition and are not able to account for the effects induced by the propagation of waves in the upper soil sections, characterised by a minor confinement. Concerning kinematic stress resultants, results of some applications available in [26] are considered as benchmarks. Applications refer to 12 m long piles with different inclination (θ = 0°, 10°, 20°, 30°) embedded in a homogeneous soil deposit characterized by shear wave velocities V_s of 250 and 110 m/s (E_p/E_s = 100, 500). The pile Young's modulus and density are E_p = 30000 MPa and ρ_p = 2.5 t/m^3, respectively. The seismic input at the ground surface is constituted by an artificial accelerogram with a peak ground acceleration a_g = 0.375g.
Figure 3 shows the envelopes of absolute values of shear forces and bending moments and the envelopes of axial forces arising along the pile because of the kinematic interaction. Benchmark shear forces are overall well reproduced, independently on the pile rake angle. However, with reference to E_p/E_s = 100 significant differences are evident in proximity of the pile head and nearby the pile base. As for bending moments, benchmarks are well reproduced expect for the local inconsistencies in proximity of the pile head where bending moments resulting from the BE approach tend to reduce, probably as a consequence of the minor degree of confinement exerted by the superficial soil. Finally, envelopes of maximum and minimum axial forces along the pile obtained from the applications show discrepancies of about 25÷30% with respect to benchmarks for both soil conditions (E_p/E_s = 100, 500), mainly concentrated in the lower half-length of the pile. Overall, the presented model provides a reliable prediction of kinematic stress resultants with only some minor inaccuracies at the pile head, where usually inertial effects, dominating the pile response, are considered for the pile design.

2.2 Simplified pseudo-static approach

A simplified procedure for the evaluation of stress resultants in single piles subjected to earthquake soil displacements is presented in this section. The procedure allows obtaining not only the peak bending moment at the interface between soil layers with impedance contrast but also the complete distribution of the stress resultants along the pile. The evaluation of the effects induced in piles by the propagation of seismic waves in the soil is studied by means of a static equivalent procedure that can be easily implemented in commercial finite element computer codes for structural analysis or simple spreadsheets. A single pile embedded in a layered soil is considered. Under the simplifying assumption that the motion of the soil deposit due to the seismic excitation is not influenced by the presence of the foundation, the pile stress resultants due to kinematic interaction are evaluated by assuming the pile as an elastic beam resting on a Winkler foundation subjected to the earthquake soil displacements evaluated by means of a dynamic response spectrum analysis of the soil deposit.
The free-field displacement profile developing in a generic soil deposit constituted by n homogeneous horizontal layers of thickness h_j because of the seismic motion applied at the underlying rigid bedrock (Figure 4) can be evaluated considering the dynamics of a shear deformable column, assuming the soil to behave linearly and considering constant elastic modulus and density within each layer. By assuming a reference system frame $\{0; z_j\}$ for each layer (Figure 4) the equation of motion for the column is given by

$$\rho_{s,j}\ddot{u}_s(z_j,t) - G_{s,j}u_s''(z_j,t) = -\rho_{s,j}\ddot{u}_b(t) \quad \text{for } j = 1,\dots n \tag{4}$$

with the relevant boundary and continuity conditions

$$\begin{aligned} &u_s'(z_1,t) = 0 && \text{for } z_1 = 0 \\ &u_s(z_j,t) = u_s(z_{j+1},t) && \text{for } j = 1,\dots n-1; z_j = h_j; z_{j+1} = 0 \\ &G_{s,j}u_s'(z_j,t) = G_{j+1}u_s'(z_{j+1},t) && \text{for } j = 1,\dots n-1; z_j = h_j; z_{j+1} = 0 \\ &u_s(z_n,t) = 0 && \text{for } z_n = h_n \end{aligned} \tag{5}$$

where $G_{s,j}$ and $\rho_{s,j}$ are the elastic modulus and density of the j-th soil layer, respectively, $u_s(z_j, t)$ denotes the horizontal relative soil displacement while $u_b(t)$ is the soil displacement at the bedrock level. By solving the associated eigenvalue problem, the soil displacement may be expressed by a linear combination of the r modes as

$$u_s(z_j,t) = \sum_{r=1}^{\infty} U_r(z_j)q_r(t) \quad \text{for } j = 1,\dots n \tag{6}$$

Substituting Equation (6) into Equation (4), multiplying by U_m (i.e. the contribution of the m-th mode), integrating over the length of the soil column and considering the orthogonality properties of the modes, yields

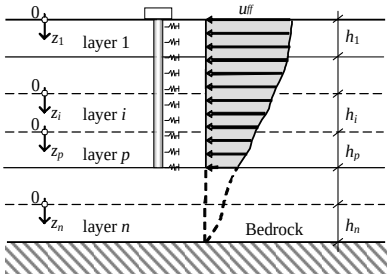

Figure 4. Horizontally layered soil profile overlying a rigid formation and pile subjected to the free-field soil displacements

$$\ddot{q}_m(t) + \omega_m^2 q_m(t) = -\Gamma_m \ddot{u}_b(t) \tag{7}$$

that, for classically damped system, transforms into

$$\ddot{q}_m(t) + 2\xi_m \omega_m \dot{q}_m(t) + \omega_m^2 q_m(t) = -\Gamma_m \ddot{u}_b(t) \tag{8}$$

In Equations (7) and (8), ω_m and Γ_m are the natural circular frequency and the modal participation factor of the *m*-th mode of vibration, respectively, while ξ_m is the relevant damping ratio. The latter represents the damping of the soil that is generally dependent on the strain level to which the ground is subjected. A constant value for the modal damping ratio for the *m*-th mode of the deposit should be determined to represent the material hysteretic damping of the whole system; thus, if energy dissipation occurs differently in each layer a weighted value of the damping ratio may be determined by empirical approaches [29]. The motion of the continuous deposit may be studied by considering an infinite number of Single Degree of Freedom (SDF) systems each one governed by Equation (8), which foresees the following solution

$$q_m(t) = \Gamma_m D_m(t) \tag{9}$$

where $D_m(t)$ is the response of the *m*-th SDF system. The peak soil displacement for the *m*-th vibration mode can be directly computed through the earthquake response spectrum by means of the expression

$$u_{ff,m}(z_j) = \Gamma_m \frac{S_a(\omega_m;\xi_m)}{\omega_m^2} U_m(z_j) \tag{10}$$

where $u_{ff,m}(z)$ is the maximum free-field displacement and $S_a(\omega_m, \xi_m)$ is the ordinate of the earthquake pseudo-acceleration response spectrum associated to the modal damping ratio ξ_m and corresponding to the vibration frequency ω_m. Furthermore, U_m is the *m*-th vibration mode. The procedure needs the solution of the eigenvalue problem associated to Equation (4), which can be easily solved separating variables *z* and *t* for the definition of the horizontal displacement $u_s(z_j, t)$ as follows:

$$u_s(z_j; t) = U(z_j) e^{i\omega t} \tag{11}$$

where $U(z_j)$ is the modal displacement function and ω is the circular natural frequency. The general solution of the problem assumes the form

$$U(z_j) = A_j cos\left(\frac{\omega}{V_{s,j}} z_j\right) + B_j sin\left(\frac{\omega}{V_{s,j}} z_j\right) \tag{12}$$

where V_{sj} is the shear wave velocity of the *j*-th soil layer and A_j and B_j are the integration constants depending on the conditions at the boundaries of each layer. Considering boundary conditions (5), a system of 2*n* homogeneous equations in the constants A_j and B_j can be obtained and natural frequencies of the system can finally be computed imposing determinant of the coefficient matrix of above system equal to zero.

The pile, which is assumed to be a Euler-Bernoulli beam with constant flexural rigidity $E_p J_p$ resting on a Winkler-type medium embedded into *p* soil layers ($1 \le p \le n$), is subjected to earthquake soil displacements (10) (Figure 4). The equilibrium condition of a generic pile element subjected to the soil displacement profile associated to the contribution of the *m*-th mode of vibration may be written in the form

$$E_p J_p u_m''''(z_j) + k_j[u_m(z_j) - u_{ff,m}(z_j)] = 0 \tag{13}$$

where u_m is the pile displacement and k_j is the Winkler coefficient of the *j*-th layer that can be derived from the literature (e.g. [30]). Solution of Equation (13) assumes the form

$$u_m(z_j) = e^{-\alpha_j z_j}(C_{1,j} cos\alpha_j z_j + C_{2,j} sin\alpha_j z_j) + e^{\alpha_j z_j}(C_{3,j} cos\alpha_j z_j + C_{4,j} sin\alpha_j z_j) + \frac{4S_m\alpha_j^4}{\beta_j^4 + 4\alpha_j^4}(A_j cos\beta_j z_j + B_j sin\beta_j z_j) \tag{14}$$

where

$$\alpha_j^4 = k_j / 4E_p J_p$$
$$\beta_j = \omega_m / V_{s,j} \tag{15}$$
$$S_m = \Gamma_m \frac{S_a(\omega_m;\xi_m)}{\omega_m^2}$$

By substituting boundary and continuity conditions at the pile ends and at the interface between the soil layers, a system of 4*p* homogeneous equations in the constants $C_{1,j}$, $C_{2,j}$, $C_{3,j}$, $C_{4,j}$ may be obtained. The solution of the system allows calculating the displacements of the pile sections and consequently the stress resultants at each depth of interest for each mode of the free-field motion. If the pile is embedded into the bedrock, supports of springs of the pile sections below the bedrock are subjected to a null prescribed motion. Since the response to earthquake is primarily due to the lower modes of vibration only the first few natural frequencies and modal shapes must be evaluated to compute the kinematic response with a good level of precision. When higher modes have to be considered the effects need to be combined with the modal Complete Quadratic Combination (CQC); details can be found in [20].

An application is presented below comparing results of the above simplified approach with those obtained by a dynamic soil-pile kinematic interaction analysis. Single piles of two diameters embedded into the three-layered soil profile reported in Figure 5a are considered. The model proposed by Dezi et al. [11] is used for the evaluation of the kinematic interaction of the selected case studies considering the soil-pile interaction and the radiation damping. The concrete piles have Young modulus $E_p = 3 \cdot 10^7$ kPa and density $\rho_p = 2.5$ Mg/m³. Piles are 24 m long and have a circular cross section of diameter d of 600 and 800 mm. A constant soil Poisson's ratio $\nu_s = 0.4$ and a constant material hysteretic damping $\xi_s = 10\%$, compatible with the strain level in the soil, are considered. The bedrock is characterized by a shear wave velocity $V_{sb} = 800$ m/s and a density $\rho_{sb} = 2.5$ Mg/m³. The seismic action is defined at the bedrock level and consists of an artificial accelerogram (Figure 5a). The first three modes have been considered for an overall effective modal mass of 86% of the total one. Contributions of each mode to the pile response are independently evaluated and then combined with the CQC.

Figure 5b shows the soil displacement profile relevant to the first three vibration modes of the soil deposit (Equation (10)) while Figure 5c depicts the relevant deformed shapes of piles (Equation (14)). Figure 6 shows comparisons between results obtained with the proposed simplified method and that resulting from the dynamic analyses. The effects induced by the contribution of only the first mode and the modal CQC of the effects produced by the first two and three modes are presented. As expected, by increasing the number of modes contributing to the response stress resultants obtained from the dynamic analyses are reproduced closer. Further details of the procedure efficiency can be found in [11].

2.3 Empirical formulas for estimating kinematic bending moments in vertical single piles

A comprehensive parametric study has been carried out to analyze the effects of kinematic interactions in vertical single piles having restrained rotational degree of freedom at the head. The objective of this study is to examine the influence of the main parameters governing the dynamic response of piles (e.g the pile diameter, the properties of the layered soil and the bedrock location), and to determine simplified formulas for the estimation of pile kinematic bending moments.

The analysis scenario covers a wide range of possible homogeneous deposits overlying or not a stiff bedrock, to also investigate effects of the layer interface on pile bending moments for highly contrasting soil properties and various pile diameters. Layouts of the investigated piles are presented in Figure 7a, b while Figure 7c reports the adopted parameters. For the homogenous soil deposit, a pile length of 24 m is considered while for soil layers overlying the bedrock, the pile length is assumed to be 48 m in order to assure a suitable embedment of the pile into the bedrock for the 42 m thick soil layer; preliminary analyses are performed to assure that the pile length does not affect the maximum kinematic bending moments attained at the layer-bedrock interface in the case of smaller thicknesses of the superficial layer. Piles are considered to have a linear elastic behaviour, with a Young's modulus $E_p = 30000$ N/mm² and a mass density $\rho_p = 2.5$ Mg/m³.

Soil-pile interaction effects are evaluated by means of an analysis procedure consisting of two steps: firstly, the free-field motion is obtained in absence of piles; secondly, the free-field motion is applied to the soil-pile system to perform the kinematic soil-pile interaction analysis.

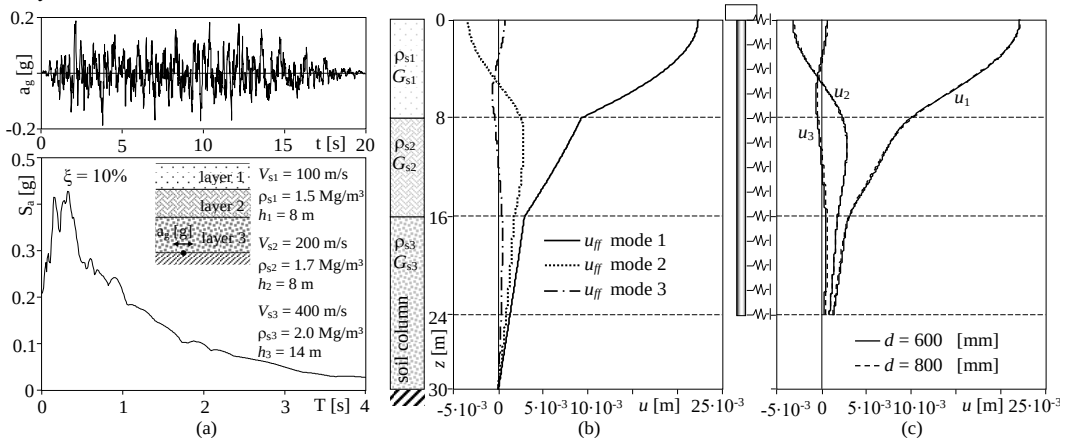

Figure 5. (a) Accelerogram and response spectrum at the bedrock level, (b) free-field maximum displacement profile, (c) pile displacements when subjected to the free-field motion.

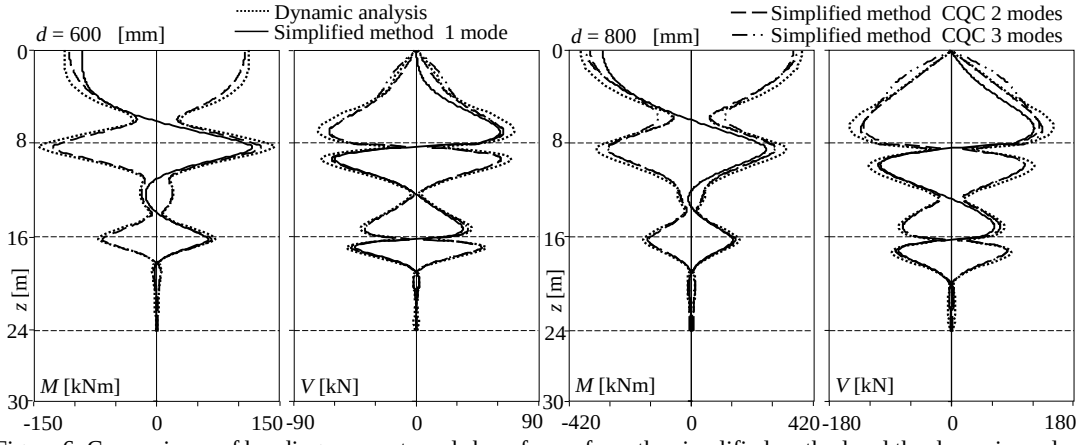

Figure 6. Comparisons of bending moments and shear forces from the simplified method and the dynamic analysis

In the first step the seismic input motion along the pile is obtained by means of a 1D local site response analysis where the seismic action at the outcropping rock is linearly deconvoluted at the bedrock level and then propagated through the soil profile [31]. In the second step the kinematic soil-pile interaction problem is investigated adopting through the numerical procedures developed by the authors [8, 11]. The seismic action at the outcropping bedrock is represented by an artificial accelerogram matching the EC8 Type 1 elastic response spectrum for ground type A [32] and Peak Ground Acceleration (PGA) 0.25*g*. Figure 8 shows the response spectra obtained from the deconvolution analyses for all the investigated soil profiles; each graph refers to a specific soil type and collects results obtained for different thickness *h* of the deformable layer. Spectral de-amplifications are overall evident in correspondence of the fundamental periods of the soil deposits: soil profiles with V_s = 400 m/s are particularly responsive to the deconvolution process in the range 0÷0.5 s where the periods of the soil deposits fall and where the spectrum of the seismic input action achieves the maximum values.

Figure 9 shows an example of the results obtained from the applications in terms of kinematic pile bending moments. Different curves in each frame refer to soil-foundation layouts (for end-bearing piles) characterized by different thicknesses of the superficial layer. For the sake of simplicity only results relevant to pile diameters d = 0.4 m and d = 1.2 m are reported, while the complete set of data are addressed in [19]. It can be observed that bending moments present peaks in correspondence of the deposit-bedrock interface and overall peaks values tend to increase by increasing the bedrock depth. Furthermore, in the case of soft soils, bending moments at the pile head tend to increase with respect to those achieved within the pile shaft.

Starting from data from the complete set of analyses, empirical formulas to predict the kinematic bending moments at the pile head, as well as at the deposit-bedrock interface, have been defined and calibrated. To this purpose, results are normalized with respect to the values obtained for the stiffer soil (V_s = 400 m/s), hereafter called M_{400}. With reference to the pile head, analyses of data revealed that (*i*) the M_{400} values are only slightly dependent on *h* whereas they are very sensitive to the pile diameter; (*ii*) for each deposit depth *h*, trends of normalised bending moments with respect to V_s are almost superimposed for the different pile diameters and are characterised by an exponential law; (*iii*) only for soft soils (V_s = 100-200 m/s) and low-depth deposits (h = 6 m) a dependency on the pile diameter is evident.

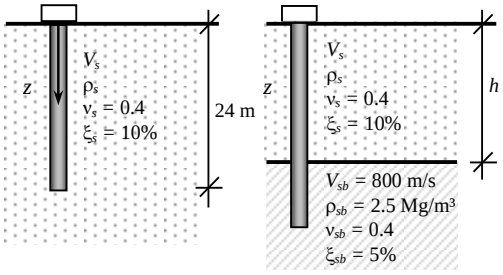

V_s [m/s]	ρ_s [Mg/m³]	d [m]	h [m]
100, 200, 400	1.5, 1.7, 2.0	0.2, 0.4, 0.6, 0.8, 1.0, 1.5, 2.0	6, 12, 18, 30, 42

(a) (b) (c)

Figure 7. Case studies: (a) layout of the homogeneous profile; (b) layout of the two-layered profile; (c) parameters

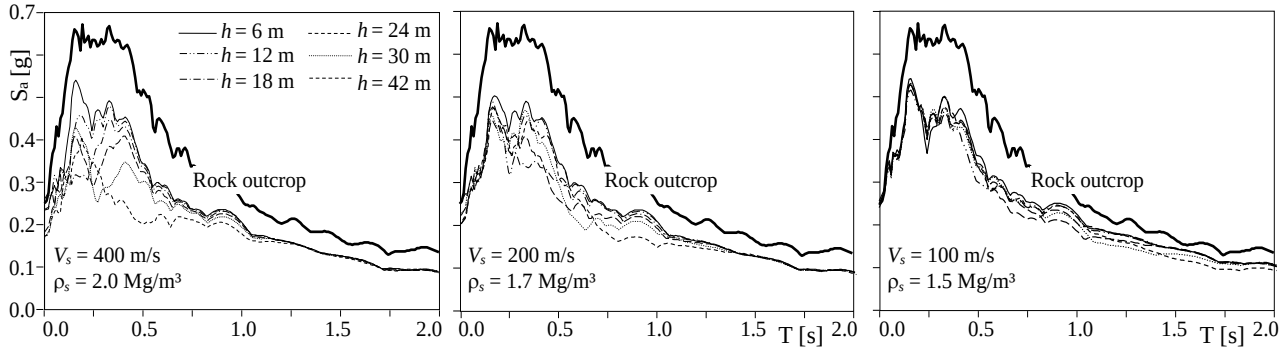

Figure 8. Response spectra at the bedrock level for all the investigated soil profiles

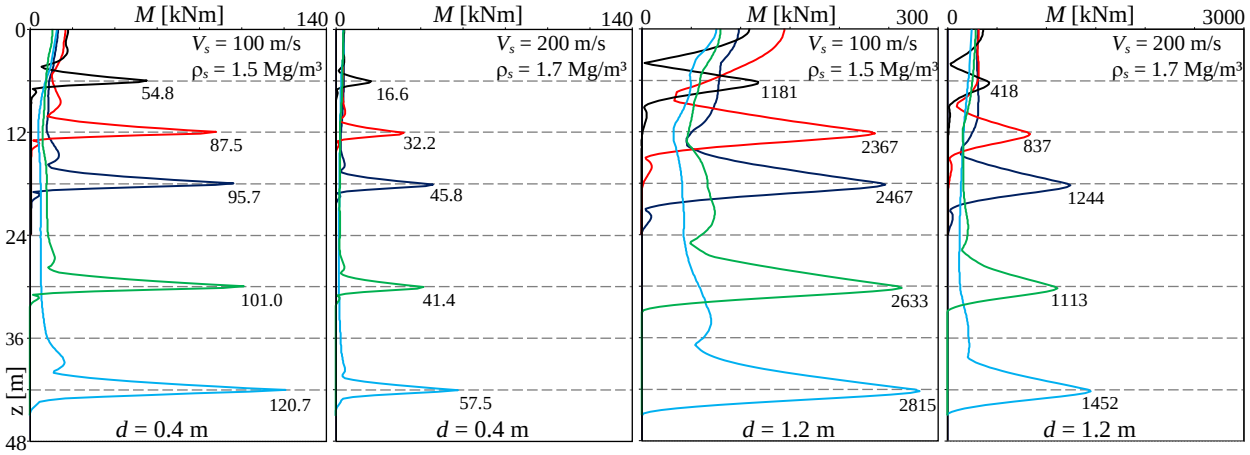

Figure 9. Piles kinematic bending moments

With reference to bending moment at the deposit-bedrock interface, analysis of data reveals that values of M_{400} are more sensitive to the deposit thickness whereas the above considerations hold for the normalised bending moments.
These remarks suggest that an empirical expression of the bending moments, both at the head and at deposit-bedrock interface, may have the following form:

$$M(V_s; d; h; \mathrm{PGA}) \cong \frac{\mathrm{PGA}}{0.25g} M_{400}(d; h) e^{f(d;h)(V_s - 400)} \tag{16}$$

where the ratio PGA/0.25g accounts for different seismic intensities owing to the problem linearity. Formulas for evaluating bending moments $M_{400}(d, h)$ and the function $f(d, h)$, defining the dependency of the exponential regression on d and h, are calibrated with a nonlinear least square procedure by fitting data obtained in the parametric analysis.
With reference to the maximum bending moment at the deposit-bedrock interface, the following polynomial approximations hold:

$$M_{400}(d; h) = (55.5d^3 + 414d^2 - 189d + 23.4)(-0.001h^2 + 0.0718h - 0.2) \tag{17}$$

$$f(d; h) = (-0.05d + 0.864)(0.000122h - 0.01103) \tag{18}$$

With reference to the maximum bending moment at the pile head, the following expressions are obtained:

$$M_{400}(d; h) = (85d^3 - 85.75d^2 + 30.93d - 3.37)(0.000133h^2 - 0.00042h + 1.091) \tag{19}$$

$$f(d; h) = (-0.07d + 1.002)(0.000067h - 0.0113) \tag{20}$$

Equation (16) allows predicting bending moments at the critical sections of an end-bearing pile embedded in a generic homogeneous soil starting from the PGA relevant to soil class A as defined in EC8 [32], the shear wave velocity of the deposit, the pile diameter and the bedrock depth. It is worth noting that Equation (16) accounts for both the local site response and the soil-pile kinematic interaction. With reference to the pile head, Figure 10a compares results obtained through Equation (16) with those of the dynamic analysis: errors are generally acceptable for design purposes. Less precision is obtained for bending moments at the head of piles with very small diameter. Figure 10b refers to the deposit-bedrock interface and adds results obtained by applying the formula of Nikolaou et al. [33] (white dots), which is only able to predict kinematic bending moments at the deposit-bedrock interface. As can be noticed, the proposed formula gives better results.

3 PILE GROUPS

3.1 Analytical approach

In this section, the numerical model developed by Dezi et al. [12] for the dynamic interaction analysis of inclined pile groups is briefly addressed. Piles are modelled with linear beam finite elements and the soil is assumed to consist of a set of independent horizontal layers of infinite extent, making use of the Winkler's assumption. The pile-soil-pile interaction and the radiation damping are formulated in the frequency domain within each layer by means of elastodynamic Green's functions available in the literature. For the model validation and some comparisons, the simplified elastodynamic solutions provided by Dobry et al. [23] and by Roesset and Angelides [34], as well as the damping model of Gazetas and Dobry [25], are herein used. The presence of a rigid cap is accounted for by constraining the displacements of the pile heads. The model allows evaluating the kinematic response of pile groups with generic number of piles, generic layout and piles inclination; in particular the motion of the piles cap and the stress resultants in piles due to the passage of harmonic shear or seismic waves in the soil may be computed; in the latter case, the incoming free field may be derived from local one dimensional or spatial analysis depending on the complexity of the site, also accounting for the nonlinear soil behaviour. Furthermore, the condensation of the problem on the rigid cap degrees of freedom allows obtaining impedances of the pile group; these may be used, in conjunction with the pile cap motion, to perform consistent soil-structure interaction analyses according to the substructure approach.

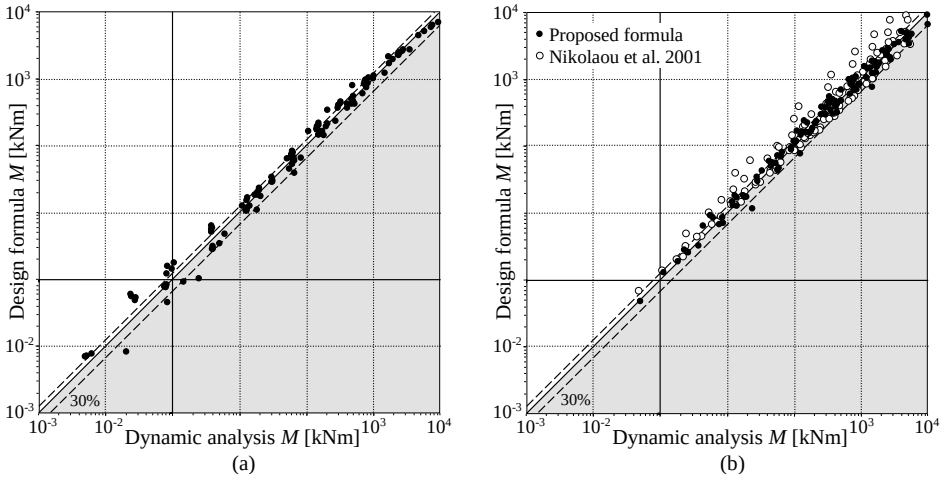

Figure 10. Comparisons of bending moments from the design formula and the dynamic analyses: (a) pile head; (b) deposit-bedrock interface

A group of n circular piles with same diameter but with different rake angles is considered and a global reference system frame $\{0; x_1, x_2; z\}$ is defined as in Figure 11a. The orientation of the generic p-th pile, that is assumed to be a Euler-Bernoulli beam, is definite by the unit vector $\mathbf{a}_{\zeta,p}$ of the pile longitudinal axis ζ_p, from which an orthonormal local reference system frame can be constructed for each pile. For the sake of simplicity, the projection of the pile length on the vertical axis z is equal to L, for all the piles. The pile group equilibrium condition may be expressed in weak form by the Lagrange-D'Alembert principle that, in the frequency domain, provides the following equation:

$$\int_0^L \mathbf{BK}\mathcal{D}\mathbf{Ru}(\omega;z)\cdot\mathcal{D}\mathbf{R}\hat{\mathbf{u}}(z)dz - \int_0^L \mathbf{r}(\omega;z)\cdot\hat{\mathbf{u}}(z)dz - \omega^2\int_0^L \mathbf{BMu}(\omega;z)\cdot\hat{\mathbf{u}}(z)dz \quad \forall\hat{\mathbf{u}}\neq\mathbf{0} \tag{21}$$

where $\mathbf{B}$ is the matrix containing the Jacobians of the coordinate transformations (from the local to the global reference frame), $\mathbf{K}$ is the stiffness matrix of the pile group, $\mathbf{u}$ is the vector collecting displacements of all piles at depth z, $\mathbf{R}$ is the overall rotation matrix obtained by assembling sub-matrixes $\mathbf{R}_p$ of each pile (providing local pile displacements from global ones), and $\mathcal{D}$ is a formal operator providing piles curvatures and normal strains from displacements. Furthermore, $\mathbf{M}$ is the mass matrix of the pile group from which inertia forces arising during the motion depend, and $\mathbf{r}$ is the vector collecting the interaction lateral forces $\mathbf{r}_p$ developing in each pile of the group (Figure 11b).
The Winkler's hypothesis, in conjunction with the compatibility condition between the pile and soil displacements, due to both the free-filed motion $\mathbf{u}_{ff}$ and the soil-pile interaction forces (Figure 11c), make it possible to express forces $\mathbf{r}$ as

$$\mathbf{r}(\omega;z) = -\tilde{\mathbf{D}}^{-1}(\omega;z)\left[\mathbf{u}(\omega;z) - \mathbf{u}_{ff}(\omega;z)\right] \tag{22}$$

where $\tilde{\mathbf{D}}$ is the complex valued matrix obtained by assembling sub-matrixes $\mathbf{D}_{pq}(\omega;z)$, expressing the soil displacements at the location of the p-th pile due to a time-harmonic unit point load acting at the location of the q-th pile. Taking Equation (22) into account, the global balance condition in weak form (21) becomes

$$\int_0^L \mathbf{BK}\mathcal{D}\mathbf{Ru}(\omega;z)\cdot\mathcal{D}\mathbf{R}\hat{\mathbf{u}}(z)dz - \int_0^L \tilde{\mathbf{D}}^{-1}\mathbf{u}(\omega;z)\cdot\hat{\mathbf{u}}(z)dz - \omega^2\int_0^L \mathbf{BMu}(\omega;z)\cdot\hat{\mathbf{u}}(z)dz = \int_0^L \tilde{\mathbf{D}}^{-1}\mathbf{u}_{ff}(\omega;z)\cdot\hat{\mathbf{u}}(z)dz \quad \forall\hat{\mathbf{u}}\neq\mathbf{0} \tag{23}$$

Differently form the single pile, for which the strong from of the balance conditions is derived, the finite element method in the displacement-based approach is used herein to solve the problem numerically, starting from the weak balance condition (23). Piles are divided into E finite elements of length L_e and the local displacements within the elements are expressed by interpolating those at the end nodes, according to standard analytical procedures. The pile cap is imposed introducing a rigid constraint for pile head nodes and defining a master node $\mathbf{d}_F$ with 6 generalized displacement components. By collecting displacements of the embedded pile nodes into vector $\mathbf{d}_E$, the following linear system can be obtained

$$\begin{bmatrix}\mathbf{Z}_{FF} & \mathbf{Z}_{FE}\\ \mathbf{Z}_{EF} & \mathbf{Z}_{EE}\end{bmatrix}\begin{bmatrix}\mathbf{d}_F\\ \mathbf{d}_E\end{bmatrix} = \begin{bmatrix}\mathbf{f}_F\\ \mathbf{f}_E\end{bmatrix} \tag{24}$$

from which the complex-valued foundation impedance matrix

$$\mathfrak{Z}(\omega) = (\mathbf{Z}_{FF} - \mathbf{Z}_{FE}\mathbf{Z}_{EE}^{-1}\mathbf{Z}_{EF}) \tag{25}$$

and the FIM

$$\mathbf{d}_F(\omega) = \mathfrak{Z}^{-1}(\mathbf{Z}_{FF} - \mathbf{Z}_{FE}\mathbf{Z}_{EE}^{-1}\mathbf{Z}_{EF}) \tag{26}$$

can be derived through simple manipulations. The FIM represents the displacements of the master node because of the free-field motion filtered by the pile group. The model has been widely tested, in terms of convergence, and validated comparing results with those obtained from refined 3D finite element model of soil-foundation systems characterized by inclined piles [12]. Both the foundation impedances, the kinematic response and the pile stress resultants have been considered in the validation process; for the sake of brevity, only few results are reported below for what concern impedances, referring to a homogeneous soil deposit and two piles configurations. Figure 12 shows the pile group layouts and compares the translational impedance of the case studies obtained from the presented model with those achieved through a refined 3D solid model. Impedances are expressed in the form $\mathfrak{Z}_i = \kappa_i + ia_0c_i$ where $a_0 = \omega d/V_s$, where d is the pile diameter and V_s is the shear wave velocity of the soil, and stiffness and damping coefficients are plotted separately; the proposed model, characterized by a very low computational effort compared to that of the 3D model, is able to predict the dynamic response of the investigated case studies with a good level of accuracy.

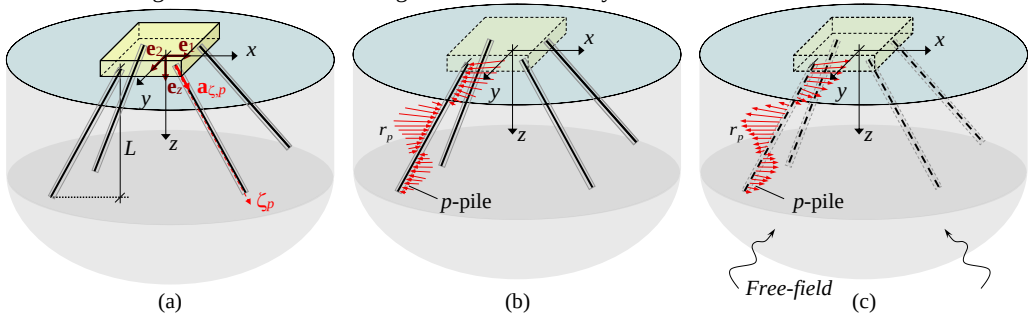

Figure 11. (a): Pile group with inclined piles; (b) foundation subjected to interaction forces and (c) soil subjected to propagating seismic waves and interaction forces

3.2 Empirical formulas for estimating kinematic bending moments in vertical pile groups

The model presented in the previous section is used to perform a comprehensive parametric investigation to analyze effects of kinematic interactions in floating and end-bearing pile groups. Like for the single pile, the objective of this study is to examine the influence of the main parameters governing the dynamic response of pile groups, and to determine simplified formulas for the estimation of pile kinematic bending moments. To this purpose a sub-set of the soil profiles previously adopted for the single pile are considered (Figure 7), limited by the assumption of a pile diameter $d = 1$ m. The pile Young's modulus and mass density are assumed to be $E_p = 30000$ N/mm² and $\rho_p = 2.5$ Mg/m³, respectively. 2x2, 3x3, 4x4 and 5x5 pile groups characterized by three different pile spacing s are considered ($s/d = 2, 3, 5$) for a total number of 39 analyses, in the case of floating piles, and 117 analyses in the case of end-bearing piles. The analysis scenarios cover a wide range of possible two-layered soil profiles and make it possible to investigate the effects of the layer interface on pile bending moments for highly contrasting soil properties. The seismic action, applied in one of the two principal directions of the pile groups, is constituted by the single artificial accelerogram adopted for the parametric investigation of single piles, so that results presented in Figure 8 hold.

With reference to end-bearing piles, post-processing of data from the applications reveals that the group effect on the maximum bending moments is evident at the pile cross sections located at the bedrock interface; with respect to results of the single fixed-head pile, bending moment in the corner pile generally reduces by increasing the number of piles constituting the group. At the piles head the group effect is less significant and reductions of the bending moments, with respect to the single pile, are evident only in the case of a surface bedrock location ($h = 6$ m). For floating piles, the kinematic bending moment arising in the corner piles of the groups is very similar to those of the single pile within the whole pile length and slight reductions are visible only in the case of soft soil ($V_s = 100$ m/s). Furthermore, by reducing the s/d ratio a decrease of the maximum bending moments at both the pile head and at the bedrock interface can be observed. Further details on the data post-processing are available in [21].

With the aim of proposing simplified empirical formulas to predict the maximum kinematic bending moment in the piles of the group (both at the pile head and at the deposit-bedrock interface), a representative set of piles is selected for each group and the relevant bending moments are normalized with respect to the one resulting from the single pile analysis.

As an example, Figures 13 shows the normalized kinematic bending moments at the pile head and at the bedrock interface for deposits with shear wave velocity $V_s = 200$ m/s and for $s/d = 3$. Dots are used to plot results of each pile while lines are adopted to connect the maximum values attained for each group, which has a practical interest from the design point of view. By increasing the number of piles constituting the group, results are generally more scattered. External piles, and particularly corner ones, are characterized by greater bending moments while inner piles are protected. With reference to the maximum values, mostly attained at corner piles, specific trends of the normalized bending moments are clearly evident at both the pile head and at the deposit-bedrock interface: with respect to single pile, increments of the kinematic bending moments at the head are observed (considering the most stressed pile of the group) by increasing the number of piles constituting the group while at the deposit-bedrock interface bending moments in the most stressed pile of the group reduces by increasing the number of piles. Furthermore, very similar curves are obtained for different shear wave velocities and bedrock locations.

By comparing the maximum normalized bending moments from all the analyses, it can be observed that, with reference to a specific s/d ratio, curves obtained for different shear wave velocities are very similar (for both the pile head and the deposit-bedrock interface), excepting those of deposits characterized by a surface bedrock ($h = 6$) for which interactions within moments arising at the head and at the bedrock interface are expected. Furthermore, moderate differences are observed by changing the s/d ratios; clearly, greater group effects are obtained for $s/d = 2$. Furthermore, the dependency of the normalized maximum bending moments on the bedrock location is slightly evident for deposits with $h = 12$ and 18 m.

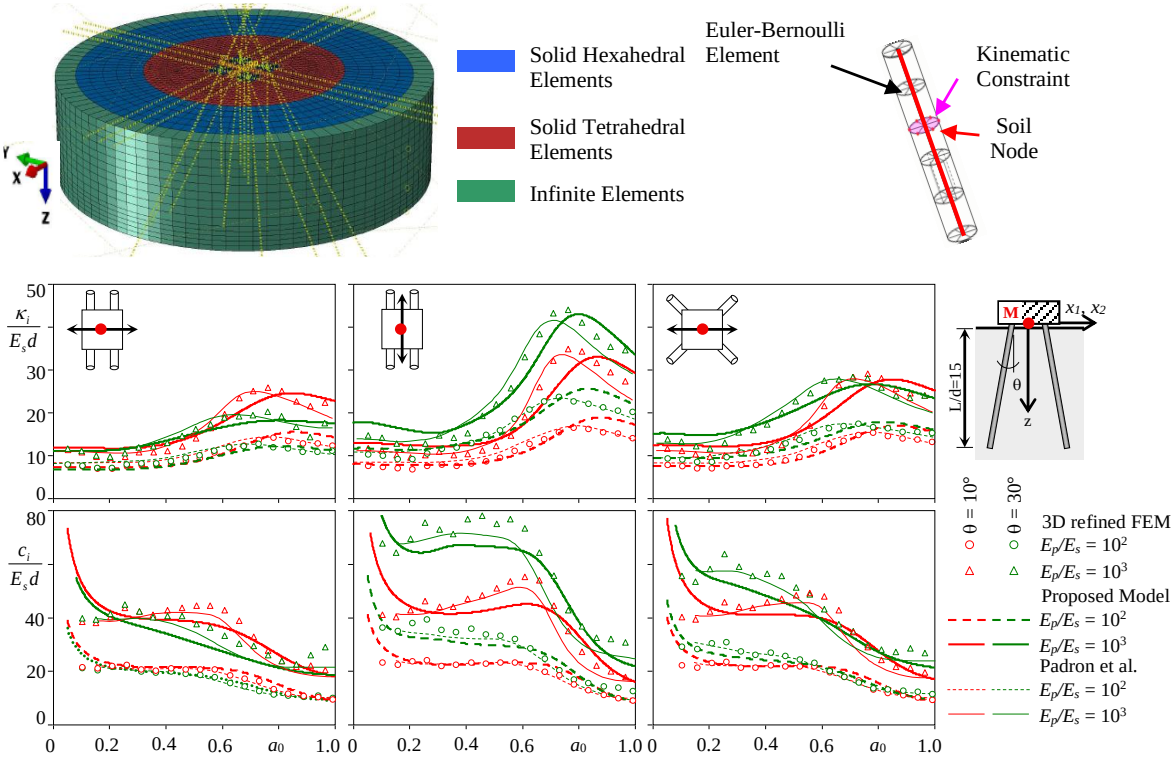

Figure 12. 3D refined finite element model and lateral dynamic impedances for inclined pile foundations in homogeneous soil

Previous remarks suggest the following empirical expression of the bending moments, both at the head and at deposit-bedrock interface:

$$M_{max}^{G} = M^{s}\alpha\left(n;\frac{s}{d}\right) \tag{27}$$

where M_{max}^{G} is the maximum bending moment arising in the piles of the group at the head or at the deposit-bedrock interface, M^{s} is the relevant single pile bending moment, α is the group factor depending on the number of piles and the pile spacing, and n is the number of pile constituting the square group. It is worth noting that Equation (27) is independent on the seismic intensity, consistently with the assumption of linear soil and pile behavior. For high levels of seismic shakings the soil nonlinear behaviour, as well as the possible formation of soil-pile gaps, have to be taken into account. However, such phenomena are expected to affect both the group and the single pile response, mitigating effects on the normalized bending moments.
The following expressions are proposed for the group factor α

$$\alpha\left(n;\frac{s}{d}\right) = a\left(\frac{s}{d}\right)log(n) + b\left(\frac{s}{d}\right) \tag{28}$$

in which coefficients a and b assume different expressions depending on the considered pile cross-sections. For the pile head

$$a = 0.16\left(\frac{s}{d}\right)^{-0.28} \qquad b = 0.58\left(\frac{s}{d}\right)^{0.23} \tag{29}$$

while for the deposit-bedrock interface

$$a = -0.12\left(\frac{s}{d}\right)^{-0.30} \qquad b = 0.88\left(\frac{s}{d}\right)^{0.04} \tag{30}$$

Figure 14 shows comparisons between the theoretical values of factor α and values resulting from Equation (27); the grey regions are those in which the application of the proposed formula will lead to underestimate the maximum bending moment in the piles of the group (assuming the results obtained from the numerical procedure as benchmarks). The errors obtained are generally acceptable for design purposes (about 10% in the grey region). The accuracy of Equation (27) is evaluated comparing results with those obtained from the analytical procedure presented in the previous section (benchmarks). All cases of the parametric investigation are taken into account and the maximum kinematic bending moments in single piles are evaluated adopting the simplified formulas for single piles and the static equivalent method discussed in the previous sections; in the latter case, only the contribution of the first vibration mode is considered. Figure 15a, b compares results from the dynamic applications with those of the simplified formulas: errors are generally acceptable for design purposes and largely compensated by the simplicity of application of the empirical proposed formulas.

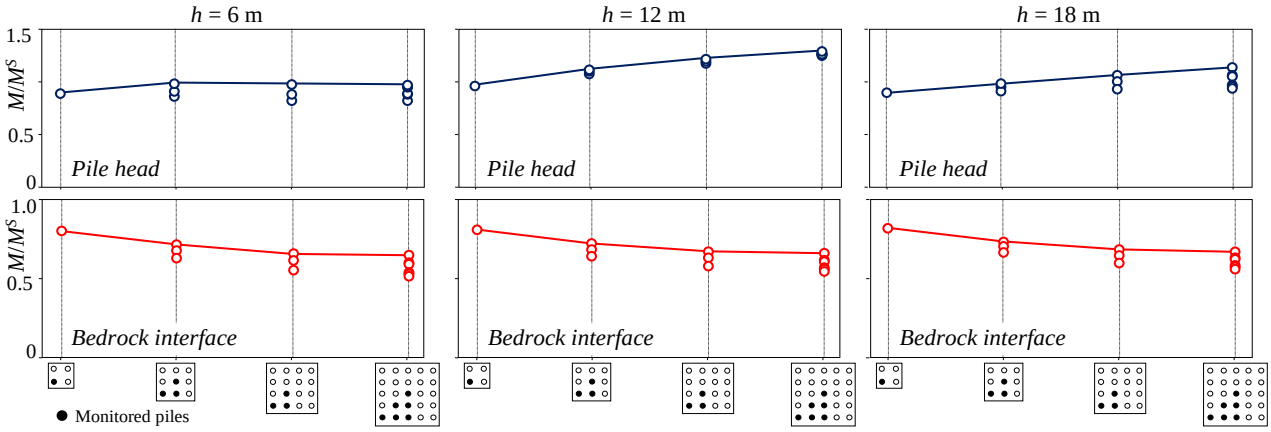

Figure 13. End-bearing piles: normalised bending moment at the pile head and at the bedrock interface for V_s = 200 m/s and s/d = 3

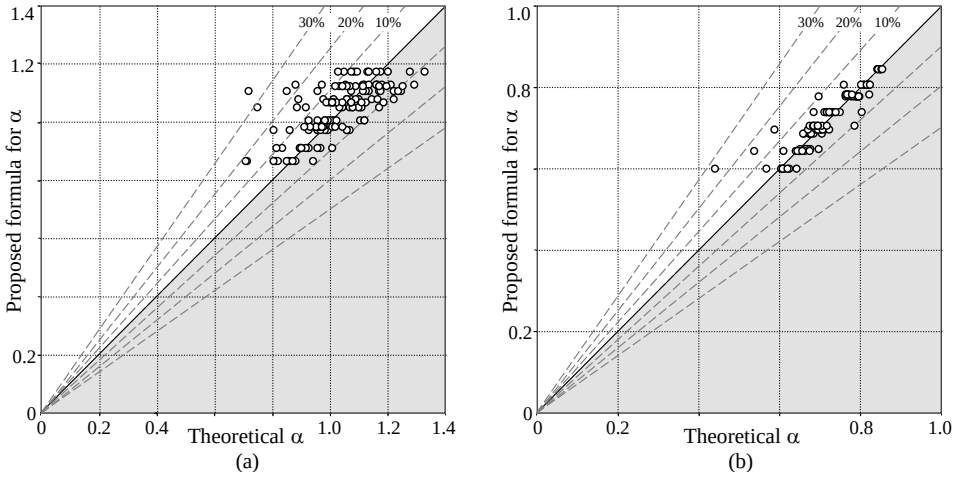

Figure 14. Comparisons of exact values of factor α and values from Equation (46): (a) pile head; (b) deposit-bedrock interface

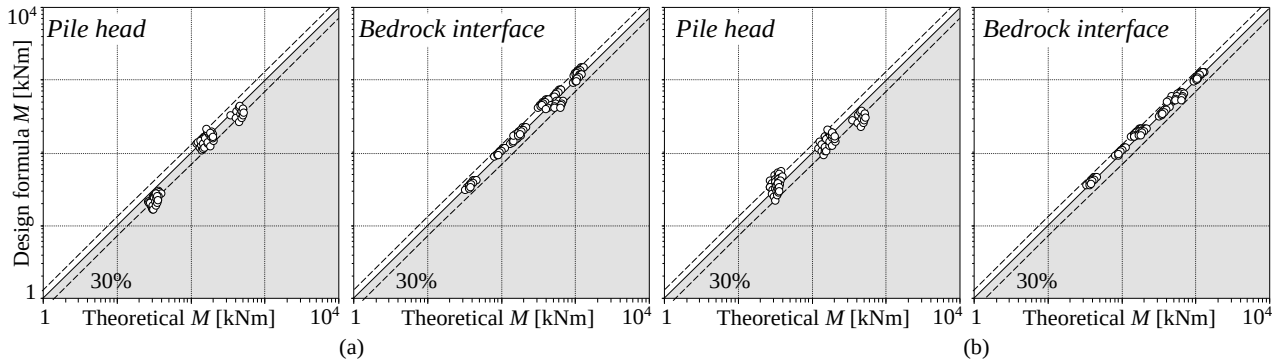

Figure 15. Comparisons of bending moments form dynamic analyses and from Equation (40): (a) M^s estimated with empirical formu las; (b) M^s estimated with the pseudo-static approach

CONCLUSIONS

A review of some analytical and numerical procedures for the dynamic analysis of soil-pile foundation systems in the framework of the sub-structure approach has been presented. Single piles and pile groups with a generic inclination and layout are considered and the relevant dynamics is formulated in the frequency domain through both analytical and numerical approaches. In addition, simplified methods for the evaluation of the kinematic interaction effects on piles are shown. The reliability of the presented tools in capturing the dynamic stiffness and the overall kinematic response of pile foundations is briefly investigated comparing results of the presented approaches with those available in the literature or achieved through refined finite element models.
From an engineering point of view, the analytical and numerical methods herein presented are recommended for performing soil-structure interaction analyses as they assure an accuracy similar to that obtained from computationally demanding 3D solid soil-foundation finite element models. On the other hand, the simplified approaches are suitable for computing kinematic interaction effects when an overall soil-structure interaction analysis is not required. Anyhow, kinematic effects on piles must be combined with those resulting from inertial interaction analyses, suitably accounting for their possible non-synchronous occurrence during earthquakes.

APPENDIX I

The analytical solution of system (2) (Section 2.1) is obtained introducing vector

$$\mathbf{x}(\omega;\zeta) = \left[\mathbf{u}_t \quad u_\zeta \quad \mathbf{u}_t' \quad u_\zeta' \quad \mathbf{u}_t'' \quad \mathbf{u}_t'''\right]^T \tag{A1}$$

which collects the unknown functions and its higher-order derivatives. Taking Equation (A1) into account, system (2) and the relevant boundary conditions (3) can be rewritten in the canonical form

$$\mathbf{x}' - \mathbf{W}(\omega)\mathbf{x} = \mathbf{c}(\omega;\zeta) \tag{A2}$$

$$\begin{aligned} &[\mathbf{D}(\omega)\mathbf{x} + \mathbf{P}(\omega)] \cdot \coprod_{1,5}^{1} \hat{\mathbf{x}}\big|_0 = 0 \ \ \forall \hat{\mathbf{x}} \\ &[\mathbf{D}(\omega)\mathbf{x} - \mathbf{P}(\omega)] \cdot \coprod_{1,5}^{1} \hat{\mathbf{x}}\big|_L = 0 \ \ \forall \hat{\mathbf{x}} \end{aligned} \tag{A3}$$

where **W** and **D** are complex valued matrices, depending on the stiffness of the pile cross section and on the impedance of the soil layers, while **c** and **P** are vectors depending on distributed soil-pile reaction forces and loads concentrated at the pile ends, respectively. The general solution of system (A2) is obtained by summing the complementary solution (solution of the associate homogeneous equation) to a particular solution depending on the external loads. It can be demonstrated that such a solution may be written as

$$\mathbf{x} = \mathbf{E}(\omega;\zeta)\mathbf{g}(\omega) + \mathbf{E}(\omega;\zeta)\int \mathbf{E}^{-1}(\omega;\zeta)\mathbf{c}\, d\zeta \tag{A4}$$

in which **E** is the exponential matrix of **B** and **g** is the vector of the integration constants that has to be calculated from the boundary conditions (A3). Equation (A2) is of general validity and the evaluation of the particular solution requires the expression of the free field motion to be known. The case of one-dimensional propagation of shear and pressure waves in the vertical direction is herein considered, which leads the following expression of vector **c**:

$$\mathbf{c} = \mathbf{Q}_h(\omega)e^{ik_h c_z \zeta} + \mathbf{T}_h(\omega)e^{ik_h c_z \zeta} + \mathbf{Q}_z(\omega)e^{ik_z c_z \zeta} + \mathbf{T}_z(\omega)e^{ik_z c_z \zeta} \tag{A5}$$

where k_h and k_z are the complex wavenumbers associated to the propagation of shear and pressure waves, respectively, while $\mathbf{Q}_h$, $\mathbf{T}_h$, $\mathbf{Q}_z$ and $\mathbf{T}_z$ are vectors of integration constants depending on the boundary conditions (i.e. at the ground surface and at the bedrock level) [8]. Considering Equation (A5), Equation (A4) yields

$$\mathbf{x} = \mathbf{E}\mathbf{g}_f(\omega) + \tilde{\mathbf{x}}_h + \tilde{\mathbf{x}}_z \tag{A6}$$

where

$$\tilde{\mathbf{x}}_h = \mathbf{E}\left[\left(ik_h c_{z\zeta}\mathbf{I} - \mathbf{W}\right)^{-1}\mathbf{E}^{-1}\mathbf{Q}_h(\omega)e^{ik_h c_{z\zeta}\zeta} - \left(ik_h c_{z\zeta}\mathbf{I} + \mathbf{W}\right)^{-1}\mathbf{E}^{-1}\mathbf{T}_h(\omega)e^{ik_h c_{z\zeta}\zeta}\right]$$
$$\tilde{\mathbf{x}}_z = \mathbf{E}\left[\left(ik_z c_{z\zeta}\mathbf{I} - \mathbf{W}\right)^{-1}\mathbf{E}^{-1}\mathbf{Q}_z(\omega)e^{ik_z c_{z\zeta}\zeta} - \left(ik_z c_{z\zeta}\mathbf{I} + \mathbf{W}\right)^{-1}\mathbf{E}^{-1}\mathbf{T}_z(\omega)e^{ik_z c_{z\zeta}\zeta}\right] \quad \text{(A7)}$$

are the particular solutions for shear and pressure waves propagating in the vertical direction, respectively, and $\mathbf{g}_f$ is the vector of the integration constants that has to be calculated from the boundary conditions. Once the solution is determined, stress resultants in the pile can be determined. For the evaluation of the soil-foundation impedances, the following homogeneous problem with non-homogeneous boundary conditions can be considered

$$\mathbf{x}' - \mathbf{W}(\omega)\mathbf{x} = \mathbf{0} \quad \text{(A8)}$$

$$\coprod_{1,5}^{1}\mathbf{x}(\omega;0) = \mathbf{x}_0$$
$$\coprod_{1,5}^{1}\mathbf{x}(\omega;L) = \mathbf{x}_L \quad \text{(A9)}$$

which, according to Equation (A4), admits solution

$$\mathbf{x} = \mathbf{E}\mathbf{g}_d(\omega) \quad \text{(A10)}$$

Substituting Equation (A10) into (A9) allows computing the vector of integration constants

$$\mathbf{g}_d(\omega) = \mathbf{G}\begin{bmatrix}\mathbf{x}_0\\ \mathbf{x}_L\end{bmatrix} \quad \text{(A11)}$$

where

$$\mathbf{G} = \begin{bmatrix}\coprod_{1,5}^{all}\mathbf{E}(\omega;0)\\ \coprod_{1,5}^{all}\mathbf{E}(\omega;\mathrm{L})\end{bmatrix} \quad \text{(A12)}$$

Finally forces at the pile head can be computed through Equations (A3)

$$\begin{bmatrix}\boldsymbol{\mathcal{R}}_0\\ \boldsymbol{\mathcal{R}}_L\end{bmatrix} = \begin{bmatrix}-\mathbf{D}\mathbf{E}(\omega;0)\mathbf{G}\\ \mathbf{D}\mathbf{E}(\omega;L)\mathbf{G}\end{bmatrix}\begin{bmatrix}\mathbf{x}_0\\ \mathbf{x}_L\end{bmatrix} \quad \text{(A13)}$$

In Equation (A13) the stiffness matrix of the pile is evident, and impedances can be finally obtained through a condensation of the stiffness matrix on the pile head displacements.

APPENDIX II

The following symbols are used in this paper:

Vectors and matrices

$\mathbf{B}$	Jacobian matrix	$C_{1,j}$, $C_{2,j}$, $C_{3,j}$, $C_{4,j}$	Integration constants
$\mathbf{c}$	Vectors of distributed forces	c	Damping coefficient
$\mathbf{D}$	Complex valued matrix	$c_{z\zeta}$	Cosine director
$\tilde{\mathbf{D}}$	Soil deformability matrix	D_m	Response of the SDF system
$\mathbf{d}$	Piles nodal displacements	d	Pile diameter
$\mathbf{E}$	Exponential matrix	E_p, E_s	Young's moduli
$\mathbf{F}_t$	Concentrated forces	E_p^*	Complex pile Young's modulus
$\mathbf{g}$	Vector of integration constants	F_ζ	Concentrated force
$\boldsymbol{\mathfrak{Z}}$	Impedance matrix	G_s	Soil elastic shear modulus
$\mathbf{J}$	Inertia matrix	h	Layer thickness
$\mathbf{K}$	Pile group stiffness matrix	I	Non-dimensional kinematic response factor
$\boldsymbol{\mathcal{K}}$	Impedance matrix of unbounded soil	J_p	Inertia about a principal axis
$\mathbf{M}_t$	Concentrated moments	k	Winkler coefficient
$\mathbf{P}$	Vectors of concentrated loads	L	Pile length
$\mathbf{Q}_h$, $\mathbf{Q}_z$	Vector of integration constants	M	Bending moment
$\mathbf{R}$	Rotational matrix	M_{400}	Bending moment for V_s = 400 m/s
$\boldsymbol{\mathcal{R}}$	Sub-vector of pile head forces	M_{max}^G	Pile group maximum bending moment
$\mathbf{r}$	Soil-pile interaction forces	M^s	Single pile bending moment
$\mathbf{T}_h$, $\mathbf{T}_z$	Vector of integration constants	q_r, q_m	Generalised displacements
$\mathbf{u}$	Pile groups displacements	S_a	Ordinate of the earthquake pseudo-acceleration response spectrum
$\hat{\mathbf{u}}$	Pile groups virtual displacements	s	Spacing of piles
$\mathbf{u}_{ff}$	Free-fields motion	U	Modal displacement function

$\mathbf{u}_h$	Pile global displacements	U_r, U_m	Modal shapes
$\mathbf{u}_t$	Pile local displacements	u_m	Pile modal displacement
$\hat{\mathbf{u}}_t$	Pile local virtual displacements	u_b	Bedrock displacement
$\mathbf{W}$	Complex valued matrix	u_s	Soil displacement
$\mathbf{x}$	Vector of unknown functions	u_z	Pile global displacement
$\hat{\mathbf{x}}$	Vector of virtual unknown functions	u_ζ	Pile local displacement
$\tilde{\mathbf{x}}_h$, $\tilde{\mathbf{x}}_z$	Particular solutions	$\hat{u}_\zeta$	Pile local virtual displacement
$\mathbf{Z}$	Stiffness sub-matrix	V_s, V_{sb}	Shear wave velocities
		x, y, z	Global reference system
Operators		α	Group factor
$\mathcal{D}$	Operator providing curvatures and strains	Γ_m	Modal participation factor
$\coprod_{i,j}^{l,m} \blacksquare$	Operator extracting segments of a matrix	θ	Pile inclination
		κ	Stiffness coefficient
Scalars		ρ_p, ρ_s, ρ_{sb}	Mass densities
A	Area	ν_p, ν_s, ν_{sb}	Poisson ratios
A_j, B_j	Integration constants	ω	Circular frequency
a_0	Non-dimentional frequency	ξ_m	Modal damping ratio
a_g	Acceleration	ξ_p, ξ_s, ξ_{sb}	Material damping ratios
a, b	Functions	ζ	Local abscissa of the pile axis

REFERENCES

[1] Novak M. Dynamic stiffness and damping of piles. Canadian Geotechnical Journal 1974; 11:574–598.

[2] Gazetas G, Dobry R. Simple radiation damping model for piles and footings. Journal of Engineering Mechanics 1984;110:937–956.

[3] Basu D, Salgado R, Prezzi M. A continuum-based model for analysis of laterally loaded piles in layered soils. Geotechnique 2009; 59(2):27–140.

[4] Nogami T, Otani J, Konagai K, Chen H. Nonlinear soil-pile interaction model for dynamic lateral motion. Journal of Geotechnical Engineering 1992;118:89–106.

[5] Tahghighi H, Konagai K. Numerical analysis of nonlinear soil-pile group interaction under lateral loads. Soil Dynamics and Earthquake Engineering 2007; 27(5):463-474.

[6] Allotey N, El Naggar MH. Generalized dynamic Winkler model for nonlinear soil–structure interaction analysis. Canadian Geotechnical Journal 2008;45:560–573.

[7] Tombari A, El Naggar MH, Dezi F. Impact of ground motion duration and soil non-linearity on the seismic performance of single piles. Soil Dynamics and Earthquake Engineering 2017; 100:72–87.

[8] Carbonari, S. Morici, M., Dezi, F., Leoni G., 2016. Analytical evaluation of impedances and kinematic response of inclined piles. Engineering Structures, 117: 384-396.

[9] Lysmer J, Udaka T, Tsai CF, Seed HB. FLUSH: a computer program for approximate 3-D analysis of soil-structure interaction problems. Report/No. EERC75–30. Berkeley: University of California; 1975 Earthquake Engineering Research Center.

[10] Padrón LA, Aznárez JJ, Maeso O. BEM–FEM coupling model for the dynamic analysis of piles and pile groups. Engineering Analysis with Boundary Elements 2007; 31(6):473-484.

[11] Dezi F, Carbonari S., Leoni G. A model for the 3D kinematic interaction analysis of pile groups in layered soils. Earthquake Engineering & Structural Dynamics 2009; 38:1281–1305.

[12] Dezi F., Carbonari S., Morici M. A numerical model for the dynamic analysis of inclined pile groups. Earthquake Engineering & Structural Dynamics 2016; 45:45–68.

[13] Wu G, Finn W. Dynamic nonlinear analysis of pile foundations using finite element method in the time domain. Canadian Geotechnical Journal 1997;34:44–52.

[14] Wakai A, Gose S, Ugai K. 3-D Elasto-Plastic Finite Element Analyses of Pile Foundations Subjected to Lateral Loading. Soils and Foundations 1999; 39 (1): 97-11.

[15] Bentley KJ, El Naggar MH. Numerical analysis of kinematic response of single piles. Canadian Geotechnical Journal, 2000; 37:1368-1382.

[16] Dobry R, O'Rourke MJ. Discussion on "Seismic response of end-bearing piles" by Flores Berrones R. and Whitman R.V. Journ. Geotech. Engng. Div. ASCE 1983; 109(5):778-781

[17] Nikolaou AS, Mylonakis G, Gazetas G, Tazoh T. Kinematic pile bending during earthquakes analysis and field measurements. Géotecnique 2001; 51(5):425-440.

[18] Dente G. Pile foundations; giudelines on geotechnical aspects for designing in seismic areas, (in Italian). Bologna, Italy: Patron Editore; 2005.

[19] Dezi F, Carbonari S., Leoni G., 2009. Kinematic bending moments in pile foundations. Soil Dynamics and Earthquake Engineering 30(3): 119-132.

[20] Dezi, F., Carbonari, S., Leoni, G., 2010. Static equivalent method for the kinematic interaction analysis of single piles. Soil Dynamics and Earthquake Engineering 30(8): 679-690.
[21] Dezi, F., Poulos, H., 2017. Kinematic Bending Moments in Square Pile Groups. International Journal of Geomechanics 17(3).
[22] Makris, N., 1997. Causal hysteretic element. Journal of Engineering Mechanics, ASCE, 123(11): 1209-1214.
[23] Dobry, R., Vicente, E., O'Rourke, M.J., Roesset, J.M., 1982. Horizontal Stiffness and Damping of Single Piles. Journal of Geotechnical Engineering Division, ASCE, 108(GT3): 439–459.
[24] Makris, N., Gazetas, G., 1993. Displacement phase differences in a harmonically oscillating pile. Geotechnique, 43(1): 135–150.
[25] Gazetas, G., Dobry, R., 1984. Simple radiation damping model for piles and footings. J. Engng. Mech., ASCE, 110(6): 937–956.
[26] Padrón, L.A., Aznárez, J.J., Maeso, O., Santana, A., 2010. Dynamic stiffness of deep foundations with inclined piles. Earthquake Engng Struct. Dynamics, 39(12): 1343-1367.
[27] Medina, C., Padrón, L.A., Aznárez, J.J., Santana, A., Maeso, O., 2014. Kinematic interaction factors of deep foundations with inclined piles. Earthquake Engng. Struct. Dynamics, 43(13): 2035-2050.
[28] Fan K., Gazetas G., Kaynia A., Kausel E., Ahmad. S., 1991. Kinematic seismic response of single piles and pile groups. J. of Geotechnical Engineering 117(12): 1860–1879.
[29] JRA (2002). Specifications for highway bridges – Part V: Seismic Design. Japan Road Association.
[30] Makris, N. & Gazetas, G., 1992. Dynamic pile-soil-pile interaction. Part II: Lateral and seismic response. Earthquake Engineering & Structural Dynamics 21, (2): 145-162.
[31] Kramer S. L., 1996. Geotechnical Earthquake Engineering. Prentice Hall, Upper Saddle River, RJ.
[32] EN 1998-1 (2004). Eurocode 8 – Design of structure for earthquake resistance – Part 1: General rules, seismic actions and rules for buildings.
[33] Nikolaou S., Mylonakis G., Gazetas G., Tazoh T. (2001). Kinematic pile bending during earthquakes: analysis and field measurements. Géotechnique, 51(5): 425–440.
[34] Roesset, J.M. and Angelides, D. 1980. Dynamic stiffness of piles; Numerical Methods in Offshore Piling: 75–82. London: Institution of Civil Engineers.